Acta Cryst. (1994). D**50**, 317–328

Refined Crystal Structure of Pseudoazurin from *Methylobacterium extorquens* AM1 at 1.5 Å Resolution

By Tsuyoshi Inoue, Yasushi Kai,* Shigeharu Harada, Nobutami Kasai and Yoshiki Ohshiro

Department of Applied Chemistry, Faculty of Engineering, Osaka University, Suita 565, *Japan*

Shinnichiro Suzuki and Takamitsu Kohzuma

Institute of Chemistry, College of General Education, Osaka University, Toyonaka 560, *Japan*

and Jiro Tobari

Department of Chemistry, College of Science, Rikkyo (St Paul's) University, Nishi-Ikebukuro, Toshima-ku 171, *Japan*

(*Received* 27 *September* 1993; *accepted* 5 *January* 1994)

Abstract

The crystal structure of pseudoazurin from *Methylobacterium extorquens* AM1 (PAZAM1) has been solved by the molecular replacement method using copper–copper distances as translation parameters, which were obtained from difference Patterson maps calculated with the synchrotron radiation data containing the multiwavelength anomalous-dispersion effect. The structure refinement was carried out by the use of molecular dynamics optimization and the restrained least-squares method. The final crystallographic R factor was 19.9% for the 14 365 reflections greater than 3σ between 1.5 and 8.0 Å resolution. This report describes the characteristic features of the structure of PAZAM1 as well as the effectiveness of synchrotron radiation for structure analysis of metalloproteins. The environment of the metal active site and the structural differences among blue-copper proteins are discussed.

Introduction

Methylobacterium extorquens AM1 is one of the methylotrophic bacteria, which grow on C_1 compounds like methylamine, formaldehyde and methanol as the sole carbon and energy source. When the bacterium is cultivated in a medium containing methylamine together with copper ions at normal concentration (< 0.1 mg l^{-1}), methylamine dehydrogenase (MADH) and a blue-copper protein named amicyanin are produced. On the other hand, when the culture medium contains copper at high concentration (> 1 mg l^{-1}), a small amount of amicyanin and large amount of another blue-copper protein named pseudoazurin are synthesized (Tobari, 1984). Pseudoazurin is quite different from amicyanin with regard to molecular weight, amino-acid sequence, and absorption and EPR spectra. Recently, MADH and amicyanin were co-crystallized (Chen, Louis, Mathews, Davidson & Husain, 1988) and the X-ray structure revealed amicyanin as the first electron acceptor from MADH (Chen *et al.*, 1993). Pseudoazurin is reported to have another location in the electron-transport chain of *Methylobacterium extorquens* AM1 growing on methylamine and excess amounts of copper (Tobari, 1984).

The amino-acid sequences of pseudoazurins from three different sources, *Methylobacterium extorquens* AM1 (PAZAM1, Ambler & Tobari, 1985), *Alcaligenes faecalis* S-6 (PAZS6; Homel, Adman, Walsh, Beppu & Titani, 1986) and *Achromobacter cycloclastes* IAM1013 (PAZIAM, Ambler, 1977), have been reported. Among these proteins, PAZS6 is the only one whose crystal structure has been determined by the X-ray diffraction method (Adman *et al.*, 1989). In this work, the molecular structure of PAZS6 was used as the initial model for the molecular replacement method to solve the crystal structure of PAZAM1.

Crystallization

PAZAM1 was purified and characterized as described previously (Ambler & Tobari, 1985). Single crystals were obtained by the hanging-drop vapor-diffusion technique with ammonium sulfate as a precipitant reagent at 293 K (Inoue *et al.*, 1991). The crystals belong to the orthorhombic system of space group $P2_12_12_1$. The unit-cell dimensions $a =$ 52.619 (4), $b = 63.280$ (6) and $c = 35.133$ (2) Å (1 Å

* Author to whom correspondence should be addressed.

Table 1. *Experimental conditions of data collection for native crystals using synchrotron radiation*

X-ray source	Synchrotron radiation (at Photon Factory, KEK, Japan)			
Camera	Sakabe's Weissenberg camera			
Detector	Imaging plate (IP; 200 × 400 mm) and BA100 system			
Crystal-to-film distance (mm)	286.5			
Collimator	0.1 mm diameter			
	Native-I		Native-II	
Wavelength, λ (Å)	1.04		1.375	
Coupling constant (° mm $^{-1}$)	2.0	2.0	2.0	2.0
Number of crystals used	1	1	1	1
Rotation axis	*b*	*c*	*a*	*c*
Oscillation angle (° sheet $^{-1}$)	11.0	13.5	14.0	10.5
Total oscillation angle (°)	209	216	196	199.5
Total exposure time (s)	522.5	540	490	498.75

Table 2. *Results of data reduction for native crystals*

Resolution range (Å)	Native-I (at λ_1 = 1.04 Å) No. of reflections observed	R_{sym} (%)	Native-II (at λ_2 = 1.375 Å) No. of reflections observed	R_{sym} (%)
15.0	131	7.0	115	9.5
15.0-7.5	1020	6.7	702	7.1
7.5-5.0	3082	7.4	2351	6.4
5.0-3.8	4096	5.8	3800	5.4
3.8-3.0	6975	6.6	6015	5.8
3.0-1.2	50881	3.9	38489	11.9
Total No. of measured reflections		94051		62302
Total No. of independent reflections		25154		19846
Total No. of reflections with anomalous dispersion		11778		9320
R_{merge}(%)		8.7		8.7

= 0.1 nm) were determined by least-squares refinement of the 2θ values of 40 reflections. The size of the unit cell indicates one pseudoazurin molecule in the asymmetric unit and 2.18 Å^3 Da^{-1} of protein. Solvent thus occupies approximately 44% of the unit-cell volume (Matthews, 1968).

Data collection

Two sets of diffraction data for the native crystal were collected with synchrotron radiation at the BL6A2 station of 2.5 GeV energy produced by the storage ring in the Photon Factory, the National Laboratory for High Energy Physics (KEK), Tsukuba, Japan. In order to perform the multi-wavelength dispersion study, intensity data were collected at two wavelengths monochromatized by an Si(111) monochromator system; the first data set (native-I) was taken at λ_1 = 1.04 Å, and the second (native-II) at λ_2 = 1.375 Å, which is just below the *K* absorption edge of the Cu atom (λ_e = 1.388 Å). Diffraction patterns were recorded on a Fuji Imaging Plate (IP, 200 × 400 mm, Fuji Photo Film) (Miyahara, Takahashi, Amemiya, Kamiya & Satow, 1986) using Sakabe's Weissenberg camera for macromolecules (Sakabe, 1991, 1983) with an aperture collimator of 0.1 mm diameter and a cylindrical cassette of 286.5 mm radius filled with helium gas. The read-out of IP data was carried out by a Fujix BA100 system (Fuji Photo Film) and the intensity data were processed using the *WEIS* program system (Higashi, 1989). R_{merge} values for the data collected at λ_1 and λ_2 were 8.7% for 25 154 reflections up to 1.2 Å resolution data, and 8.7% for 19 846 reflections up to 1.2 Å resolution data, respectively. The experimental conditions and the results of data collection with synchrotron radiation are shown in Tables 1 and 2, respectively.

Another three sets of intensity data from a native crystal (native-III) and two heavy-atom derivatives (deriv-U and deriv-Pt) were measured on a single-crystal diffractometer. A platinum derivative was obtained by soaking native crystals in a solution containing 5 m*M* K_2PtCl_4 for one day, while a uranium derivative was obtained at first by transferring the native crystal to ammonium acetate buffer solution containing 70% saturated ammonium sulfate and then to a solution containing 10 m*M* $UO_2(AcO)_2$ for 1 d. Data was collected from these crystals on a Rigaku four-circle diffractometer with β-filtered Cu $K\alpha$ radiation from a rotating anode X-ray generator (40 kV, 200 mA). A summary of the intensity measurements is shown in Table 3.

Table 3. *Results of data collection for native-crystal and heavy-atom derivatives using a Rigaku four-circle diffractomator*

	Native-III	Deriv-U	Deriv-Pt
No. of crystals used	1	1	1
No. of observed reflections*	14375	7050	9822
No. of independent reflections	13902	6474	8793
Maximum 2θ value (°)	54.2	33.7	38.2
Resolution (Å)	1.68	2.70	2.35
Total radiation damage (% in F)	5.4	10.0	8.0

* Intensity data were measured by the ω-scan method using Cu $K\alpha$ radiation (40 kV, 200 mA, β-filter).

Structure determination

The crystal structure analysis of PAZAM1 involved by the following steps.

(I). The position of the Cu atom in the native crystal was determined from the difference Patterson maps with anomalous dispersion data (native-I, λ = 1.04 Å, and native-II, λ = 1.375 Å).

(II). The position of the Cu atom was confirmed in the electron-density maps phased by two heavy-atom derivatives (native-III, deriv-U and deriv-Pt).

(III). Based on the position of the Cu atom, the molecular replacement method was carried out by the use of the *MERLOT* program package (Fitzgerald, 1988). The rotation parameters were calculated using the *CROSUM* (Crowther, 1972) function. The initial translation parameters were set to the same distance between two copper sites in the native crystal and in the model structure. The rotation and translation parameters thus obtained were refined using the *RMINIM* (Ward, Wishner, Lattman & Love 1975) function.

I. *Determination of copper site*

The difference Patterson maps in the Harker sections with coefficients of (*a*) $[F(\lambda_1)^+ - F(\lambda_1)^-]^2$, (*b*) $[F(\lambda_1)^+ - F(\lambda_2)^-]^2$ and (*c*) $[F(\lambda_2)^+ - F(\lambda_2)^-]^2$ were calculated with the synchrotron data up to 6.0 Å resolution, where F^+ and F^- stand for the structure amplitudes of Bijvoet-related reflections, and λ_1 and λ_2 correspond to the X-ray wavelengths of 1.04 and 1.375 Å, respectively. Fig. 1 shows three Patterson maps in the Harker section of $V = 1/2$ with the respective coefficients. Among a small number of noisy peaks the highest single peak appears in Fig. 1(*a*), which corresponds to the highest peaks in other Harker sections and was assigned to the copper cross vectors. The position of the Cu atom thus determined was at $x = 0.27$, $y = 0.26$ and $z = 0.60$ in fractional coordinates of the unit cell. The position was also confirmed in the Patterson maps of Figs. 1(*b*) and 1(*c*), although the corresponding peaks are not as high as the peaks in Fig. 1(*a*). After the refinement of Cu^{2+} positional parameters, phases were calculated by the multiwavelength anomalous-dispersion (MAD) method using the Cu atom as a

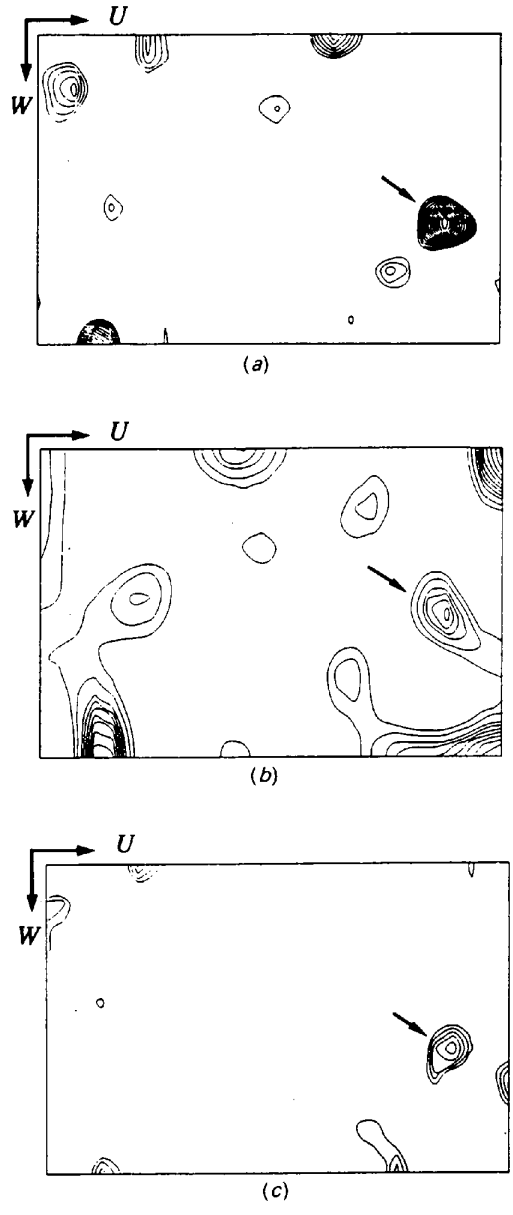

Fig. 1. Patterson maps of pseudoazurin (V = 1/2) with coefficient (*a*) $[F(\lambda_1)' - F(\lambda_1)^-]^2$, (*b*) $[F(\lambda_1)' - F(\lambda_2)]^2$, (*c*) $[F(\lambda_2)' - F(\lambda_2)]^2$, where λ_1 and λ_2 correspond to 1.375 and 1.04 Å, respectively. The positions of the Cu atom self-vectors are marked by arrows.

heavy atom against the 10 205 reflections between 10.0 and 4.0 Å resolution. An occupancy of 0.80 (23.3/29) with a B factor of 19.6 Å^2 and a figure of merit of 0.41 was obtained. Even though the calculated electron density on mini maps revealed the β-barrel structure, the confirmation of the residues was so difficult that the model building was not processed.

II. *Confirmation of copper site by the multiple isomorphous replacement (MIR) method*

After scaling the diffractometer data from the native and two heavy-atom derivatives, the mean differences in the isomorphous structure factors were calculated as 27% for the uranium derivative and 13% for the platinum derivative, respectively. The difference Patterson maps were obtained with the coefficient $(F_{PH} - F_P)^2$, where PH and P stand for the heavy-atom derivative and the native crystals, respectively. From the difference Patterson maps using deriv-U and native-III data at 5 Å resolution two major binding sites of the U atom were found, while in the corresponding maps using deriv-Pt and native-III data only few broad peaks were recognized. The determination of the absolute coordination of the U atom was performed by difference Fourier synthesis. The phases for the uranium derivative were calculated by the single isomorphous replacement method and the figure of merit obtained was 0.68 as shown in Table 4. The 3 Å resolution electron-density maps were calculated in the form of mini maps. Although some residues in the loop region were difficult to trace, all residues belonging to eight β-strands were traced easily, especially around the copper site. From the electron-density maps, the copper site, the highest peak in the whole map, was analyzed to be at $x = 0.27$, $y = 0.26$ and $z = 0.60$, which was identical to the copper position determined in step (I).

III. *Molecular replacement method*

The crystal structure of PAZAM1 was finally determined by the molecular replacement method using the *MERLOT* (Fitzgerald, 1988) program package. The molecular structure of PAZS6 (Adman *et al.*, 1989) was used as the starting structure model. The atomic coordinates were obtained from the Protein Data Bank. The Cu atom in PAZS6 was located on an origin point of a 100 × 100 × 100 Å primitive cell and the structure factors were calculated up to 3.2 Å resolution. The cross-rotation function was first calculated with the data between 13 and 3.2 Å resolution in the *CROSUM* (Crowther, 1972) function and each set of rotation parameters thus obtained was used sequentially to calculate the

Table 4. *Heavy-atom parameters of the uranium derivative*

U-atom site		Site 1	Site 2
Fractional coordinates	x	0.031	0.485
	y	0.053	0.688
	z	0.477	0.299
B_{iso} (Å^2)		20.6	21.1
Occupancy (%)		16.6	10.1
R_K (%)		13.3	
Figure of merit		0.68	

R value in the *RMINIM* (Ward *et al.*, 1975) function. In the *RMINIM* calculations the molecular translational parameters were fixed to the position of the Cu atom in PAZAM1 which was obtained independently by the MIR and MAD methods. The fifth-highest peak ($\alpha = 45.0$, $\beta = 76.0$, $\gamma = 195.0°$) and the translation parameters yield a minimum R factor after five cycles of minimization in the *RMINIM* function. After several cycles of subsequent refinement, the best positional parameters gave an R factor of 53.9%; the final Euler angles were $\alpha = 48.80$, $\beta = 77.61$, $\gamma = 193.89°$ and the final translation parameters were $x = 0.2814$, $y = 0.2620$, $z = 0.5944$. The initial atomic coordinates for the current structure were generated by using these parameters in the *ROTTRN* function.

Refinement

Refinement protocol

Refinement of the crystal structure of PAZAM1 was carried out using both a stereochemically restrained least-squares refinement method (*PROLSQ*, Hendrickson & Konnert, 1981) and the simulated-annealing refinement method which involves molecular dynamics optimization (*X-PLOR*, Brünger, Kurian & Karplus, 1987). The refinements were carried out on an NEC EWS 4800/220 for *PROLSQ* and on an IRIS 4D 25GT for *X-PLOR*. Model building was performed on IRIS using the program *FRODO* (Jones, 1978). Both $2F_o - F_c$ and difference Fourier maps as well as omit maps were used throughout.

The first step of the refinement was performed using *X-PLOR* Version 2.2 (Brünger, Krukowski & Erickson, 1990). By using prepstage refinement, the R factor decreased from 51.6 to 33.3% with 2.5 Å resolution data, and by simulated-annealing calculations at 3000 K, the R factor became 23.9% in the data range from 5 to 2.5 Å resolution. The resulting $2F_o - F_c$ electron-density map was continuous except for a residue at the C-terminal end. Three further steps of refinement were performed by *X-PLOR* using stepwise-increased data. Consequently, the molecular dynamics refinement brought the R factor

Table 5. *Results of the slow-cooling refinement (X-PLOR Version 2.2)*

Step	Resolution range (Å)	Weight (kcal mol $^{-1}$)	Check R (%)	Check CPU (s)	Prepstage R (%)	Prepstage CPU (s)	Slowcool Temp. (K)	Slowcool R (%)	Slowcool CPU (s)
1	5.0–2.5	41464	51.6	675	33.3	3720	3000	23.9	60456
2	5.0–2.5	46750	38.8	624	24.3	1604	4000	23.6	57028
3	5.0–2.0	57501	40.4	644	28.4	406	4000	26.6	90311
4	5.0–2.0	53669	39.6	675	27.1	2171	4000	26.0	84986

Table 6. *Results of the refinement progress by PROLSQ*

Stage	Resolution range (Å)	No. of atoms	No. of parameters	No. of waters	No. of reflections	No. of cycles	R factor (%) Initial	R factor (%) Final
1	5.0–2.0	938	3753	0	9250	12	25.9	22.5
2	5.0–1.8	938	3753	0	9601	4	25.7	22.9
3	5.0–1.5	938	3753	0	13710	4	27.6	24.6
4	8.0–1.5	938	3753	0	14365	10	29.1	26.6
5	8.0–1.5	999	3997	61	14365	10	28.6	23.3
6	8.0–1.5	1052	4209	114	14365	13	27.2	22.0
7	8.0–1.5	1070	4281	132	14365	12	26.7	19.9

to 26.0% with data up to 2.0 Å. The results of the slow-cooling refinement by *X-PLOR* are summarized in Table 5.

Because of the ambiguity for the energy constraint parameters of metal atoms used in the molecular dynamics refinement, a somewhat unreliable copper geometry was obtained. In order to obtain exact copper geometry no restraint was imposed on the copper coordination in the final stage of refinement by *PROLSQ*. Table 6 shows the results of seven stages of the refinement process by *PROLSQ*. Every stage includes model improvement followed by several cycles of refinement. Model improvement was carried out based on the Fourier maps calculated with coefficients of $(2F_o - F_c)\exp(2\pi i\alpha_{calc})$ and $(F_o - F_c)\exp(2\pi i\alpha_{calc})$.

Water molecules were added in three separate steps by the use of the *PEAK* program (Okamoto & Hirotsu, unpublished) to select peaks on the $F_o - F_c$ maps followed by the program *WATER* (Okamoto & Hirotsu, unpublished work) to assign water molecules to the peaks with reasonable distances for both water–protein and water–water interactions. A total of 132 water molecules were included in the final structure model and further rebuilding and cycles of refinement for the water structure finally reduced the R factor to 19.9%.

Refinement summary

The refined crystal structure includes 4281 protein atoms (non-H atoms), one metal ion and 132 water molecules. The last cycle of the refinement with 14 365 unique reflections in the range 8.0–1.5 Å resolution gave a crystallographic R factor of 19.9% with quite reasonable stereochemistry. The root-mean-square (r.m.s.) deviations from standard values

Table 7. *Final refinement statistics*

Resolution range (Å)	8.0–1.5
No. of reflections	14365
Completeness (8.0–1.5 Å) (%)	75.5
Total number of atoms (non-H)	4281
Solvent atoms (non-H)	132
R factor (8–1.5 Å) (%)	19.9
Average B factors (Å^2)	
Main chain	12.9
Side chain	13.8
Solvent	32.4
Root-mean-square deviation from standard values	
Bonds (1—2 distance) (Å)	0.024
Angles (1—3 distance) (Å)	0.039
Dihedral angles (1—4 distance) (Å)	0.044

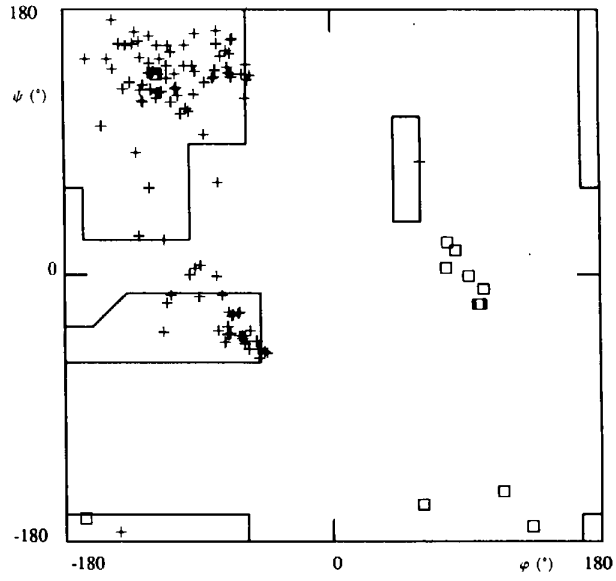

Fig. 2. Ramachandran plot of the final model of PAZAM1. Glycine residues are marked with squares.

are 0.024 Å for bond distances (1—2 distance), 0.039 Å for angle distances (1–3 distance) and 0.044 Å for dihedral angles (planar 1—4 distance). Table 7 gives the final refinement statistics. A Ramachandran plot is given in Fig. 2. Because there are few residues outside the allowed regions, the current model is considered to have good stereochemistry. The r.m.s. error of the atomic positions estimated by a Luzzati plot (Luzzati, 1952) is between 0.10 and 0.15 Å, but the structure of the copper site is so rigid and its electron density is so clear that the error may be much less for the copper-coordination geometry.

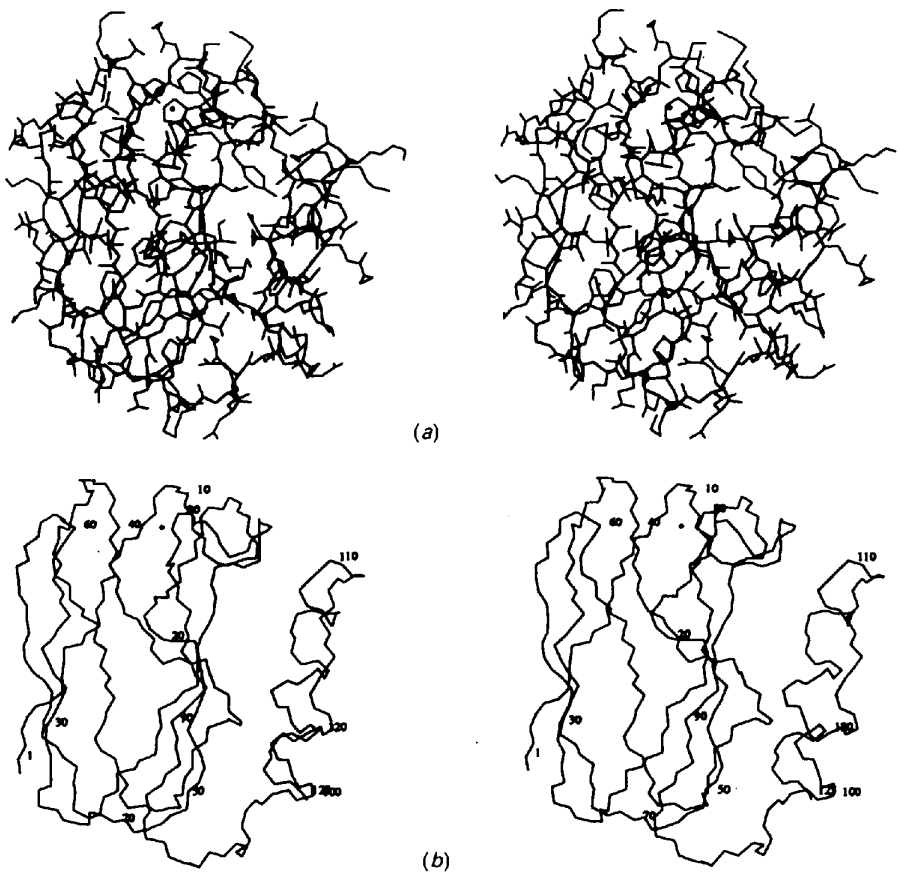

Fig. 3. Stereoviews of the overall structure of PAZAM1. (*a*) All the non-H atoms excluding water molecules, and (*b*) backbone structure of pseudoazurin, are shown together with the Cu atom, which is represented by a dot.

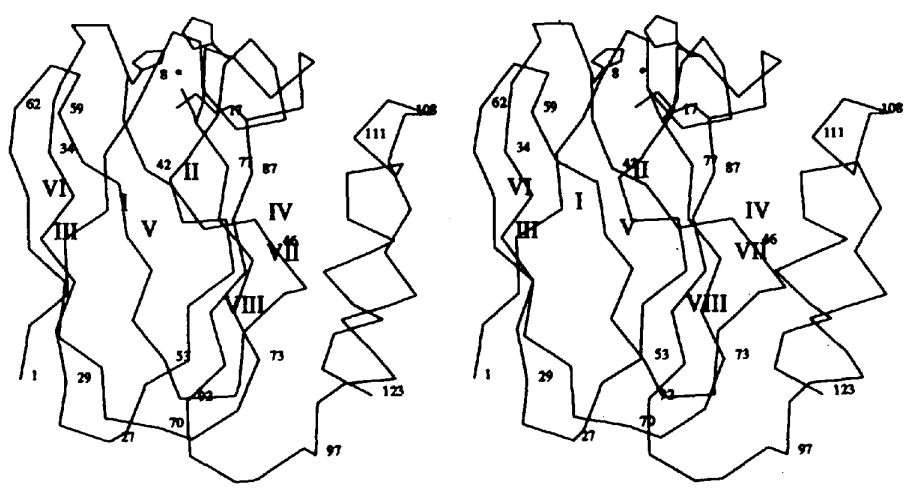

Fig. 4. A stereoview of the topological structure of PAZAM1. The overall structure is an eight-stranded β-barrel which forms two β-sheets. One is composed of strands I, II, III and VI, and the other consists of strands IV, V, VII and VIII. The Cu atom shown by a dot is located at the north end of the molecule.

Results

Three-dimensional structure

The complete model for all non-H atoms of PAZAM1, excluding water molecules, is shown in Fig. 3(*a*), while the backbone structure is shown in Fig. 3(*b*). The approximately spherical pseudoazurin molecule has overall dimensions $38 \times 38 \times 27$ Å^3, which is almost the same as the starting model of PAZS6 used as the starting structural model in the molecular replacement method. The molecule of PAZAM1 has a β-barrel structure formed by eight strands. Fig. 4 is a stereo figure showing the C_α atoms of the whole structure. Each strand consists of 5–11 residues: I, 1–8; II, 17–27; III, 29–34; IV, 40–46; V, 53–59; VI, 62–70; VII, 73–77; VIII, 87–92. Residues 97–108 and 111–123 make two α-helices. The β-barrel is built up by two β-sheets; one is formed by strands I, II, III and VI, and the other is formed by strands IV, V, VII, and VIII. The topology of 'Greek key', which is generally accepted in a protein formed by a β-barrel, is also found when the barrel is opened between strands II and VIII.

The 'kink' structure in strand II, which is peculiar to the starting model, is also confirmed in the electron-density map with the coefficient of $2F_o - F_c$ and also in the omit map. This structure contains a dislocation in the middle of β-strand II, but the gap is stabilized by hydrogen bonds between strands I and II or strands II and VIII.

The overall structural features found in PAZAM1 are common to those in the blue-copper proteins such as plastocyanin (Guss & Freeman, 1992), azurin (Baker, 1988) and amicyanin (Chen *et al.*, 1993). Although the amino-acid sequences are considerably different from other blue-copper proteins, it is very interesting that the topologies in these blue-copper proteins are quite similar.

Fig. 5. Stereoview of the backbone structures of PAZAM1 and PAZS6 superimposed. PAZAM1 is shown with thick lines, PAZS6 with thin lines. A total of 740 atoms were matched (370 atoms for PAZAM1 and 370 atoms for PAZS6) and the r.m.s. error is 1.41 Å.

The whole structure of PAZAM1 is similar to that of PAZS6 used as the starting model in the structure analysis. The proportion of identical residues is 55/123 (45%) between these pseudoazurins. Fig. 5 shows the superimposed structures of PAZAM1 and PAZS6. The two structures are so analogous that the averaged r.m.s. deviation between two backbone structures is only 1.41 Å.

Copper environment

(1) *Copper site*. The Cu atom is located near the top surface of the molecule (Fig. 4). One of the four copper ligands (His81), however, projects from the molecular surface above the Cu atom. The distance between the Cu atom and the molecular surface is about 6 Å. Four ligands located in the middle of two

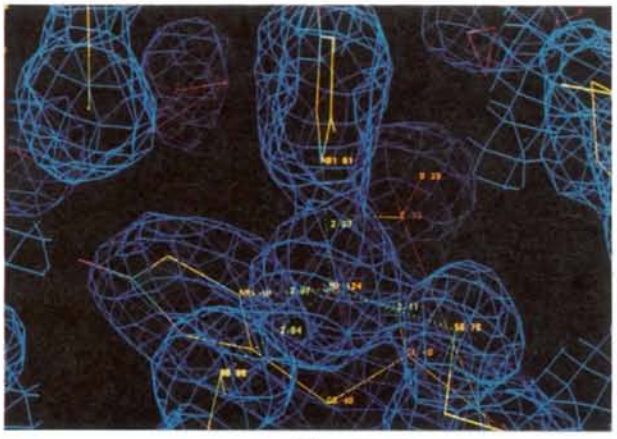

(*a*)

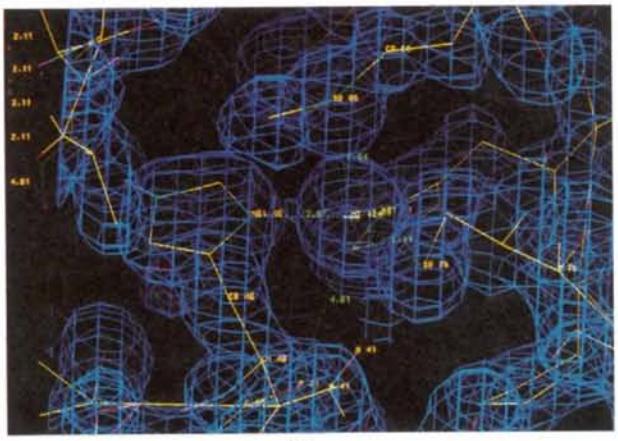

(*b*)

Fig. 6. Electron-density maps calculated at 1.5 Å resolution around the Cu atom in pseudoazurin. (*a*) The geometry of the Cu atom is clearly a distorted tetrahedral structure formed by four ligands (H40, C78, H81, M86), and (*b*) the ligand Cys78 is bent from the tetrahedral structure by the conserved NH···S hydrogen bond.

Table 8. *Geometry around the metal in some typical blue-copper proteins*

Distances (Å)

	N_δ of His (1)	S_γ of Cys (2)	N_δ of His (3)	S_γ of Met (4)	O atom
PAZAM1*	2.07	2.15	1.97	2.66	4.03
PAZS6†	2.20	2.14	2.27	2.67	3.99
PCY‡	2.04	2.13	2.10	2.90	3.82
AZA§	2.08	2.12	2.01	3.12	3.16

Angles (°)

	1—Cu—2	1—Cu—3	1—Cu—4	2—Cu—3	2—Cu—4	3—Cu—4
PAZAM1*	143.8	93.8	85.8	110.1	108.6	111.8
PAZS6†	138.4	100.0	86.3	111.7	107.0	108.8
PCY‡	132.1	96.6	85.4	122.9	108.1	102.7
AZA§	135.3	100.9	78.8	121.6	109.5	93.5

* Pseudoazurin from *Methylobacterium extorquens* AM1.
† Pseudoazurin from *Alcaligenes faecalis* S-6.
‡ Plastocyanin from poplar leaf.
§ Azurin from *Alcaligenes denitrificans* NCTC8582.

β-sheets surround the active site of the Cu atom like other blue-copper proteins. One of the ligands (His40) is contained in strand IV, but the others (Cys78, His81 and Met86) are located in the loop region between strands VII and VIII. These four amino-acid residues are conserved in the blue-copper proteins except stellacyanin.

(2) *Copper coordination of PAZAM*1. Figs. 6(*a*) and 6(*b*) show the electron-density maps with the coefficient of $2F_o - F_c$ around the Cu atom calculated at 1.5 Å resolution. From these maps the coordination parameters of the Cu atom could be calculated and are listed in Table 8. The distances between the Cu atom and four ligands in PAZAM1 are 2.07 Å for $N_{\delta1}$(His40)—Cu, 2.15 Å for S_γ(Cys78)—Cu, 1.97 Å for $N_{\delta1}$(His81)—Cu and 2.66 Å for S_γ(Met86)—Cu. Meanwhile, the angle parameters between the Cu atom and these ligands in PAZAM1 range from a minimum of 86° to a maximum of 144°. From these structural parameters the geometry of the Cu atom in PAZAM1 is also confirmed to have a distorted tetrahedral structure like that of PAZS6.

Comparison with other blue-copper proteins

(1) *Copper coordination geometries*. The similar properties in all blue-copper proteins such as absorption and ESR spectra are thought to be a result of the four conserved ligands of the Cu atom. The slight difference in these properties may result from the small deformations of the coordination geometries around the Cu atom. Table 8 shows a comparison of the copper coordination with other typical blue-copper proteins; one is azurin from *Alcaligenes denitrificans* NCTC8582 (AZA, Baker, 1988) and the other is plastocyanin from the poplar leaf (PCY, Guss & Freeman, 1992). In the structure of AZA the S_γ(Met121)—Cu distance elongates to 3.12 Å, while the O atom of glycine approaches the Cu atom up to 3.16 Å. These two atoms locate on both sides of the base plane formed by three other ligands containing two histidines and a cysteine. The copper coordination in AZA was reported as the distorted trigonal bipyramidal structure (Baker, 1988). This coordination geometry of the Cu atom is also confirmed in the structure of azurin from *Achromobacter xylosoxidans* NCIB11015 (Inoue *et al.*, 1994). In PAZAM1, however, the O atom of Gly39 is located 4.03 Å from the Cu atom and the interaction of the glycine with the Cu atom is non-existent as in the structure of PAZS6. The metal coordinations of both PAZAM1 and PAZS6 are distorted tetrahedra. In the structure of PCY the carbonyl O atom of proline corresponding to glycine in PAZAM1 and the S_γ atom of methionine are located at distances of 3.82 and 2.90 Å from the Cu atom, respectively. Since the carbonyl O atom of proline may be free from interaction with the Cu atom, plastocyanin also has a distorted tetrahedral structure like pseudoazurin.

The geometrical difference around the Cu atom between PAZAM1 and AZA is also reflected in the positional deviation of the Cu atom from the base plane containing the N_δ atoms of two histidine ligands and the S atom of a cysteine ligand. In the case of PAZAM1, the Cu atom deviates by 0.39 Å from the plane towards the side of methionine. This value is very close to that of PAZS6 (0.38 Å). On the other hand, the corresponding distances for plastocyanin and azurin are 0.34 and 0.18 Å, respectively. From these parameters as well as the copper coordination geometries, the metal-site structure of pseudoazurin is found to be very close to that of plastocyanin rather than that of azurin.

(2) *Direct interactions involving hydrogen bonding to the ligand atom*. It is possible that the ligand conformation around the copper is affected by the various interactions with the neighbouring groups within the copper coordination sphere such as amino

residues or water molecules of crystallization. The interaction of the copper ligands with the amino residues includes two modes: one is a direct interaction with the ligand atom which causes the slight change of the orientation of the copper ligand and the other is an indirect interaction to modify the effect.

With regard to the direct interaction of neighboring groups with the copper ligands, two amide protons of Asn41 and His81 could possibly hydrogen bond to the ligand S atom of Cys78 in PAZAM1 as shown in Fig. 7. The N—S distances between Cys78 and Asn41 or His81 are 3.58 and 3.67 Å, respectively. The angles for hydrogen bonds are 103.2° for Cu—S—N(Asn41) and 93.8° for Cu—S—N(His81). From these parameters, the first hydrogen bond from the residue of Asn41 is fairly strong and may affect the orientation of the ligand cysteine, while the second NH···S hydrogen bond from His81 is rather weak.

Fig. 8 and Table 9 show a comparison of the mode of the conserved NH···S hydrogen bond in PAZAM1 with other typical blue-copper proteins. In AZA two NH···S hydrogen bonds are formed between Asn47 or Phe114 and the S atom of the cysteine ligand; the N···S distances are 3.52 and 3.50 Å, respectively. The Cu—S—N(amide N atom) angles are calculated as 103.8° for Asn47 and 115.4° for Phe114. Both amide N atoms locate below the base plane and interact with the S atom of cysteine ligand from its underside. On the other hand, in the structures of PCY or PAZS6 the NH···S hydrogen bond between the cysteine ligand and the conserved aspargine residues is fairly strong to fix the S atom, but the second NH···S hydrogen bond to the amide group of the histidine is rather weak (Table 9). It is unclear whether the second NH···S hydrogen bond significantly interacts with the S atom or not, but the geometrical differences among three typical blue-copper proteins may result from the difference in the orientation of the second NH···S hydrogen bond in AZA and that in other blue-copper proteins.

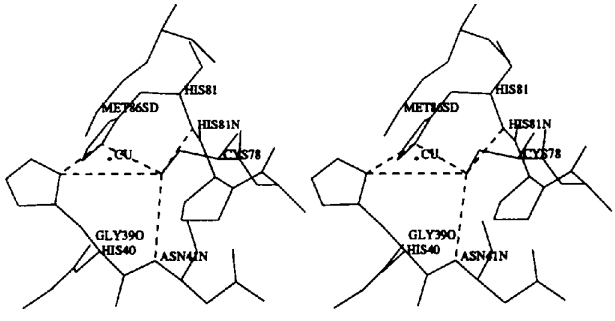

Fig. 7. Stereoview of the metal-site structure in PAZAM1. Two NH···S hydrogen bonds are observed between the ligand S atom of Cys78 and the main-chain NH groups of Asn41 or His81.

Fig. 9 shows a comparison of the amino-acid sequences from Tyr74 to Met86 in PAZAM1 together with the corresponding sequences in PCY and AZA. Phe114 is conserved in all types of azurin, while in both pseudoazurin and plastocyanin a proline residue is in the position corresponding to Phe114 in AZA. Asn41 in PAZAM1, which is next to the first histidine ligand, is conserved in all pseudoazurins, and the corresponding residue is also conserved in all blue-copper proteins as Asn38 in plastocyanins and as Asn47 in azurins. These aspargine residues offer a hydrogen bond (NH···S) to the cysteine S atom from the downside of the base plane. A pair of histidine or phenylalanine and aspargine residues contained in a β-strand may be important for inducing geometrical distortion in the copper geometry.

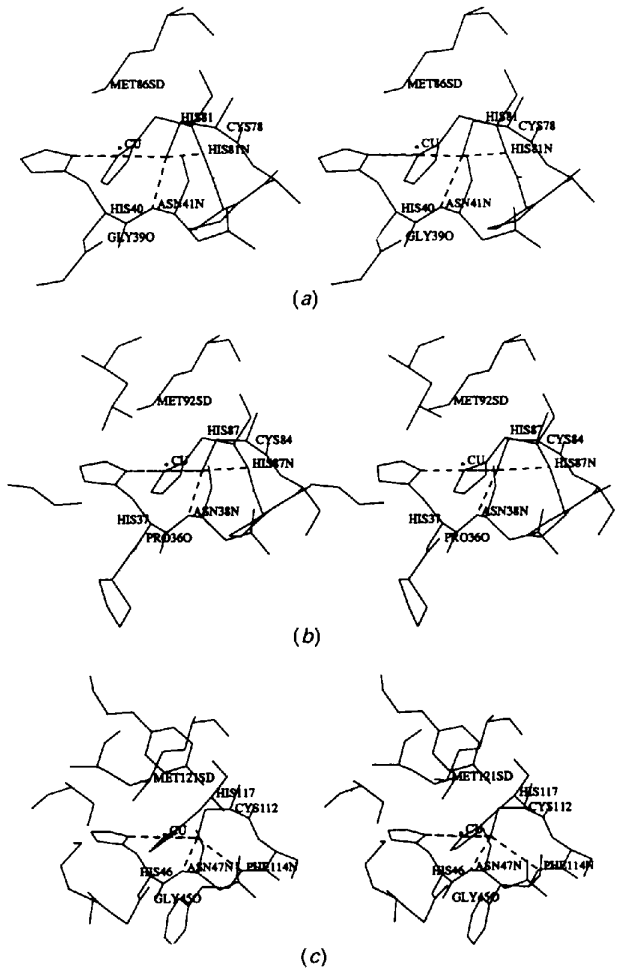

Fig. 8. Comparison of the metal-site structures among the typical blue-copper proteins: (*a*) PAZAM1, (*b*) PCY, (*c*) AZA. Stereoviews are projected along the equatorial plane defined by two histidine N_δ and cysteine S copper ligands. Dashed lines show the NH···S hydrogen bonds around the S atom of the cysteine ligand.

Table 9. *Comparison of the bond lengths and angles of the* NH···S *hydrogen bonds around Cys*78

In PAZ and PCY, N(1) and N(2) correspond to the amido group of the conserved Asn and His, repectively. In AZA, N(1) and N(2) correspond to that of the conserved His and Phe, respectively.

	Bond lengths (Å)		Angles (°)					
	S—N(1)	S—N(2)	Cu—S—C_β	Cu—S—N(1)	Cu—S—N(2)	C_β—S—N(1)	CB—S—N(2)	N(1)—S—N(2)
PAZAM1	3.59	3.68	106.4	103.2	93.8	103.1	103.1	143.1
PAZS6	3.68	3.80	105.8	104.0	89.0	109.6	96.6	145.7
PCY	3.41	4.19	109.7	109.5	86.3	110.4	96.0	141.2
AZA	3.52	3.50	106.7	103.8	115.4	107.1	119.2	103.3

(3) *Indirect interaction of the hydrogen bond with the copper geometry.* An indirect interaction has also been reported between two histidine ligands through the hydrogen bonds including a water–water bridge in both the X-ray structures of PAZS6 and PCY, but in AZA this type of water–water bridge was not found. In PAZAM1, the carbonyl O atom of Asn9 is located 2.70 Å from the His40 $N_{\varepsilon 2}$ (Fig. 10). Asn9 exists in the loop region between β-strands I and II and is placed under constraint only by a water molecule (Water 153) which is located at a distance of 2.66 Å from Asn9. In order to form the water–water bridge between Asn9 and His81, water molecule 153 must interact with another water molecule around His81 $N_{\varepsilon 2}$. The electron density was, however, so weak that the second water molecule around the His81 $N_{\varepsilon 2}$ was not located in the electron-density map. Thus, the hydrogen bond of Asn9 to His40 has little possibility of changing the direction of the ligand histidines in PAZAM1.

The conserved Asn41 residue in PAZAM1 not only hydrogen bonds with the ligand S atom of Cys78 but also with Ala79. The second hydrogen bond between Asn41 and Ala79 may indirectly affect the direction of the ligand S atom of Cys78. Ala79 in PAZAM1 is replaced by threonine in another two pseudoazurins. In the structure of PAZS6 the hydrogen bond between Asn41 and Thr79 was reported to fix the loop containing three ligands to β-strand IV. The effect of the replacement of alanine with threonine is, however, considered to be quite small since the visible spectra of PAZAM1 and PAZS6 are quite similar to each other.

Baker & Adman suggested that the slight differences of the absorption curves between azurin and pseudoazurin or plastocyanin resulted from the different number of the hydrogen bonds able to affect the coordination geometry of the Cu atom or the electronic charge on Cys78 S_γ. Since both pseudoazurin and plastocyanin have only one NH···S hydrogen bond in contrast to the two of azurin, modification of the absorption spectra may occur (Baker, 1988; Adman *et al.*, 1989).

From the detailed structural comparisons among blue-copper proteins, we consider the most significant reason for the subtle difference in the visible absorption is whether the O atom of glycine serves as the copper ligand or not. As observed in the structures of two pseudoazurins and plastocyanin, when

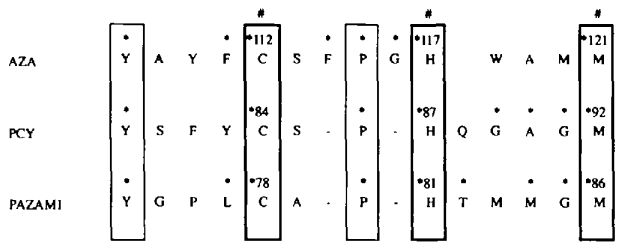

Fig. 9. Comparison of the amino-acid sequences in the loop region near the Cu atom. Three typical blue-copper proteins, pseudoazurin from *Methylobacterium extorquens* AM1 (PAZAM1), azurin from *Alcaligenes denitrificans* NCTC8582 (AZA) and plastocyanin from poplar leaf (PCY) are compared. # shows the ligand residue of the Cu atom and * shows the conserved amino acid in the same kinds of proteins.

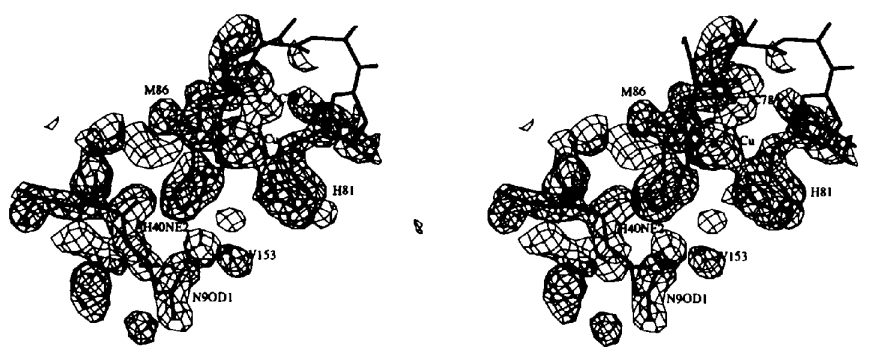

Fig. 10. Electron-density map ($2F_o - F_c$) around the ligand His81 showing the hydrogen bond between His40$N_{\varepsilon 2}$ and $O_{\delta 1}$Asn9. This O atom also hydrogen bonds to the water 153. In AZA and PCY this water molecule forms the water–water bridge between two ligand histidines.

the carbonyl O atom of glycine is located over 3.8 Å from the Cu atom, the protein absorbs at 600 nm, while if the carbonyl O atom approaches the Cu atom like in AZA the protein absorbs at 625 nm. This is related to the fact that the Cu atom selects either a tetrahedral or a trigonal bypyramidal structure. In the case of two excessive amino residues existing in the loop region between strands VII and VIII in AZA two strong NH···S hydrogen bonds are formed under the base plane of the trigonal bypyramidal structure. On the other hand, the lack of two amino residues may change the mode of the second NH···S hydrogen bond to the cysteine ligand and a tetrahedral structure is formed as in PAZAM1 and PCY.

Protein–protein interaction

From the structural information of the MADH and amicyanin complex, the active site of copper is surrounded by nine hydrophobic residues containing one histidine ligand. Pseudoazurin also has a hydrophobic area around the copper active site. The interior of pseudoazurin is hydrophobic, while the surface is relatively polar. The opposite side of the copper active center is mainly surrounded by positively charged residues (Fig. 11). The aromatic residues lie from the hydrophobic end to this positively charged region. Among them the residue Tyr82, the next residue of the ligand His81, is located at the surface of the protein. This residue is surrounded by some basic residues. This may be the reason why the recognition of the electron donor and the acceptor occurs at these two places; one is the hydrophobic area around the ligand His81 exposed on the molecular surface and the other is the basic patch around Tyr82. However, the electron-transfer pathway in the bacterium *Methylobacterium extorquens* AM1 has not been determined yet. It is a problem for the future to elucidate the pathway for electron transfer in blue-copper proteins as well as to see why pseudoazurin grows instead of amicyanin when using a high concentration of copper in growth media.*

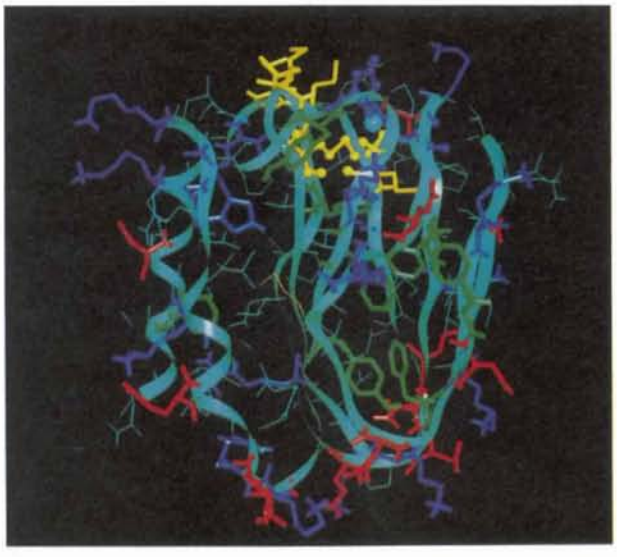

Fig. 11. Distribution of the amino-acid residues in the structure of PAZAM1. Blue residues are the basic amino acids, red shows the acidic amino acids and green shows the aromatic amino acids. The Cu atom is located at the top of the molecule (blue ball) and a hydrophobic patch which consists mainly of methionine (yellow residues) is formed around the Cu atom. H atoms are partially included based on the geometrical calculations.

The present work was partially supported by a Grant-in-Aid for Scientific Research on Priority Areas No. 03241215, 04225216 and 05209216 from the Ministry of Education, Science and Culture, Japan. The authors are grateful to the Crystallographic Research Center, Institute for Protein Research, Osaka University, for the use of its facilities. We are also grateful to Professor N. Sakabe and Dr A. Nakagawa of the National Laboratory for High Energy Physics (KEK) for the technical support during the SR data collection. And we also thank Professor K. Hirotsu and Mr A. Okamoto of Osaka City University for kindly supplying the programs *PEAK* and *WATER*.

* Atomic coordinates and structure factors have been deposited with the Protein Data Bank, Brookhaven National Laboratory. Free copies may be obtained through The Technical Editor, International Union of Crystallography, 5 Abbey Square, Chester CH1 2HU, England (Supplementary Publication No. SUP 37114). A list of depositied data is given at the end of this issue.

References

ADMAN, E. T., TURLEY, S., BRAMSON, R., PETRATOS, K., BANNER, D., TSERNOGLOU, D., BEPPU, T. & WATANABE, H. (1989). *J. Biol. Chem.* **264**, 87–99.

AMBLER, R. P. (1977). *The Evolution of Metalloenzymes, Metalloproteins and Related Materials*, edited by G. J. LEIGH, pp. 100–118. London: Symposium Press.

AMBLER, R. P. & TOBARI, J. (1985). *Biochem. J.* **232**, 451–457.

BAKER, E. N. (1988). *J. Mol. Biol.* **203**, 1071–1095.

BRÜNGER, A. T., KRUKOWSKI, A. & ERICKSON, J. W. (1990). *Acta Cryst.* A**46**, 585–593.

BRÜNGER, A. T., KURIAN, J. & KARPLUS, M. (1987). *Science*, **235**, 458–460.

CHEN, L., LOUIS, W. L., MATHEWS, F. S., DAVIDSON, V. L. & HUSAIN, M. (1988). *J. Mol. Biol.* **203**, 1137–1138.

CHEN, L., MATHEWS, F. S., DAVIDSON, V. L., TGONI, M., RIVETTI, C. & ROSSI, G. (1993). *Protein Sci.* **2**, 147–154.

CROWTHER, R. A. (1972). *The Molecular Replacement Method*, edited by M. G. ROSSMANN, pp. 173–185. New York: Gordon and Breach.

FITZGERALD, P. M. D. (1988). *J. Appl. Cryst.* **21**, 273–278.

GUSS, J. M. & FREEMAN, H. C. (1992). *Acta Cryst.* B**48**, 790–811.

HENDRICKSON, W. A. & KONNERT, J. H. (1981). *Biomolecular Structure, Function, Conformation and Evolution*, edited by R. SRINIVASAN, Vol. 1, pp. 43–57. Oxford: Pergamon Press.

HIGASHI, T. (1989). *J. Appl. Cryst.* **22**, 9–18.
HOMEL, S., ADMAN, E. T., WALSH, K. A., BEPPU, T. & TITANI, K. (1986). *FEBS Lett.* **197**, 301–304.
INOUE, T., KAI, Y., HARADA, S., KASAI, N., SUZUKI, S., KOHZUMA, T. & TOBARI, J. (1991). *J. Mol. Biol.* **218**, 19–20.
INOUE, T., NAKANISHI, H., KOYAMA, S., KAI, Y., HARADA, S., KASAI, N., OHSHIRO, Y., SUZUKI, S., KOHZUMA, T., IWASAKI, H. & SHIDARA, S. (1994). In preparation.
JONES, T. A. (1978). *J. Appl. Cryst.* **11**, 268–272.
LUZZATI, V. (1952). *Acta Cryst.* **5**, 802–810.
MATTHEWS, B. W. (1968). *J. Mol. Biol.* **33**, 491–497.
MIYAHARA, J., TAKAHASHI, K., AMEMIYA, Y., KAMIYA, N. & SATOW, Y. (1986). *Nucl. Instrum. Methods Phys. Res. A*, **246**, 572.
SAKABE, N. (1983). *J. Appl. Cryst.* **16**, 542–547.
SAKABE, N. (1991). *Nucl. Instrum. Methods Phys. Res. A*, **303**, 448–463.
TOBARI, J. (1984). *Microbial Growth on* C1 *Compounds*, edited by R. L. CRAWFORD & R. S. HANSON, pp. 106–112. Washington: American Society for Microbiology.
WARD, K. B., WISHNER, B. C., LATTMAN, E. E. & LOVE, W. E. (1975). *J. Mol. Biol.* **98**, 161–177.